Journal of Environmental Chemical Engineering 12 (2024) 114323

Contents lists available at ScienceDirect

Journal of Environmental Chemical Engineering

journal homepage: www.elsevier.com/locate/jece

Influence of design and operational parameters of a Taylor flow reactor on the bioconversion of methane to ectoines

Raquel Herrero-Lobo [a,b], Andrés Felipe Torres Franco [a,b], Wendy Mylene Llamas-Ramos [a,b], Víctor Monsalvo [c], Patricia Zamora [c], Frank Rogalla [c], Raquel Lebrero [a,b], María del Rosario Rodero [a,b], Raúl Muñoz [a,b,*]

[a] Institute of Sustainable Processes, University of Valladolid, Dr. Mergelina s/n., Valladolid 47011, Spain
[b] Department of Chemical Engineering and Environmental Technology, University of Valladolid, Dr. Mergelina s/n., Valladolid 47011, Spain
[c] Aqualia, Innovation and Technology Department, Avda. Camino de Santiago, 40, Madrid 28050, Spain

ARTICLE INFO

Keywords:
Ectoine
High mass-transfer reactor
Hydroxyectoine
Methane bioconversion
Methanotrophic consortium

ABSTRACT

Ectoine is one of the most attractive bioproducts due to its high market price and applications. Methanotrophic bacteria can synthesize ectoine from biogas. In this work, key design and operating parameters were optimised to maximise the bioconversion of methane to ectoine in a novel Taylor Flow bioreactor. This bioreactor configuration is characterized by higher gas-liquid mass transfer coefficients compared to conventional bubble column bioreactors. Thus, the influence of the internal gas recirculation flow rate (1.0 $L \cdot min^{-1}$, 2.5 $L \cdot min^{-1}$, 4.0 $L \cdot min^{-1}$, 5.5 $L \cdot min^{-1}$) at 60 and 120 min of gas residence time (GRT), the liquid recirculation flow rate (0 $L \cdot h^{-1}$, 141 $L \cdot h^{-1}$, 165 $L \cdot h^{-1}$, 395 $L \cdot h^{-1}$, 434 $L \cdot h^{-1}$) and the capillary length (1.50 and 0.75 m) was evaluated using a mixed methanotrophic consortium. Process operation at 120 min of GRT and 5.5 $L \cdot min^{-1}$ of gas recirculation flow rate enhanced methane bioconversion, resulting in a maximum efficiency of 83.8 ± 2.7 %. The decrease in capillary length from 1.5 to 0.75 m did not enhance methane bioconversion. Intracellular ectoine and hydroxyectoine reached maximum contents of 105.1 ± 8.6 $mg_{EC} \cdot g_{TSS}^{-1}$ and 33.4 ± 11.7 $mg_{HE} \cdot g_{TSS}^{-1}$, respectively. *Nitratireductor* was the dominant genus, while *Methylomicrobium* and *Methylophaga* were the main methanotrophic bacteria detected in the consortium. This study confirmed the feasibility of bioconverting novel renewable feedstocks such biogas into high-added value bio-products, boosting the circular and carbon neutral economy in bio-based industries.

1. Introduction

Ectoine (2-methyl-1,4,5,6-tetrahydropyrimidine-4-carboxylic acid) is one of the most relevant bioproducts in new biorefinery concepts due to its high market price (600–1000 €·kg^{-1}) and multiple applications [1,2]. Ectoine is a cyclic amino acid produced intracellularly by some halophilic microorganisms to maintain osmotic balance in saline environments. In addition, it is capable of protecting and stabilising macromolecules such as DNA, lipids and proteins, enzymes and cells against adverse conditions such as non-optimal temperature, radiation, freezing, desiccation and high salinity [3,4].Therefore, ectoine has applications in pharmaceutical, cosmetic and medical industries as an ingredient in nasal sprays and hair and skin care products. On the other hand, hydroxyectoine (5-hydroxy-2-methyl-1,4,5,6-tetrahydropyrimidine-4-carboxylic acid) is a hydroxylated derivative of ectoine, which exhibits even better stabilisation capacities and is also synthesized by ectoine-producers [1].

Nowadays, industrial ectoine production is carried out through the strain *Halomonas elongata* (wild type or mutant) by fermentation of high-quality carbon substrates in a high-salinity medium [1,5]. An osmotic downshock is carried out to allow the microorganisms to release the intracellular ectoine into the medium and recover it for further purification [1,6]. This process requires expensive substrates, such as glucose and sodium glutamate, and entails significant operational expenses due to the necessity of maintaining stringent sterile conditions and the high costs associated with downstream processing [2,7]. For this reason, new biorefinery concepts rely on using methanotrophic microorganisms, which can synthesise ectoine and hydroxyectoine by using methane from biogas or diffuse emissions as a carbon and energy source. This approach promotes greater environmental sustainability by leveraging biogas, a feedstock derived from the anaerobic digestion of a wide range

* Corresponding author at: Institute of Sustainable Processes, University of Valladolid, Dr. Mergelina s/n., Valladolid 47011, Spain.
E-mail address: raul.munoz.torre@uva.es (R. Muñoz).

https://doi.org/10.1016/j.jece.2024.114323
Received 11 June 2024; Received in revised form 19 September 2024; Accepted 30 September 2024
Available online 2 October 2024

Nomenclature

$A_{capillary}$	area of each capillary considering a diameter of 3 mm (m^2)
CH_4- BC	Bioconversion capacity of methane (g $CH_4 \bullet m^{-3} \bullet h^{-1}$)
CH_4-BE	Bioconversion efficiency of methane (% CH_4)
EC	Intracellular ectoine concentrations ($mg_{EC} \bullet gTSS^{-1}$)
GRT	Gas Residence Time (min)
H	Henry's law constant
HE	Intracellular hydroxyectoine concentrations ($mg_{HE} \bullet gTSS^{-1}$)
IC	Dissolved inorganic carbon (g $C_{inorg} \bullet L^{-1}$)
$IC_{L,IN}$	inorganic carbon concentrations in the fresh MSM (g $C_{inorg} \bullet L^{-1}$)
$IC_{L,OUT}$	inorganic carbon concentrations in the culture broth (g $C_{inorg} \bullet L^{-1}$)
Lc	Capillary length (m)
$m_{CH4,IN}$	inlet mass flow rates of methane (g $CH_4 \bullet h^{-1}$)
$m_{CH4,OUT}$	outlet mass flow rates of methane (g $CH_4 \bullet h^{-1}$)
$m_{CO2,IN}$	inlet mass flow rates of carbon dioxide (g $CO_2 \bullet h^{-1}$)
$m_{CO2,OUT}$	outlet mass flow rates of carbon dioxide (g $CO_2 \bullet h^{-1}$)
MSM	Mineral Salt Medium
MW_C	Atomic mass of carbon (g $C \bullet mol^{-1}$)
MW_{CO2}	Atomic mass of carbon dioxide (g $CO_2 \bullet mol^{-1}$)
Nc	Number of capillaries (25 tubes)
OD	Optical density
PCO_2	Volumetric CO_2 production rate (g $CO_2 \bullet m^{-3} \bullet h^{-1}$)
PVC	Polyvinyl chloride
$Q_g$rec	Gas recirculation flow rate ($L \bullet min^{-1}$)
Q_l	Liquid recirculation flow rate ($L \bullet h^{-1}$)
$Q_{gas\ reactor}$	Total gas flow rate that enter in the Taylor flow bioreactor ($m^3 \bullet s^{-1}$)
$Q_{liquid\ reactor}$	Total liquid flow rate that enter in the Taylor flow bioreactor ($m^3 \bullet s^{-1}$)
$Q_{L,MSM}$	Fresh mineral salt medium exchange flow rate ($L \bullet h^{-1}$)
TN	Dissolved total nitrogen (g $N \bullet L^{-1}$)
TOC	Dissolved total organic carbon (g $C_{org} \bullet L^{-1}$)
TSS	Total Suspended Solid concentration (g $TSS \bullet L^{-1}$)
V_{gas}	Gas velocity per capillary ($m \bullet s^{-1}$)
V_{liquid}	Liquid velocity per capillary ($m \bullet s^{-1}$)
$V_{reactor}$	Reactor liquid volume (m^3)
Y_{CO2}	CO_2 production yield (g $CO_2 \bullet g\ CH_4^{-1}$)

of organic wastes and wastewaters. In addition, this alternative process proves more profitable than biogas conversion into electricity and heat, which currently faces lower competitiveness compared to electricity generation by solar or wind power [8].

Many studies have demonstrated the ability of methanotrophic microorganisms to synthesize high amounts of intracellular ectoine in high-salinity media. For example, [9] achieved ectoine contents up to 108.7 ± 4.8 mg•g biomass^{-1} with a halophilic consortium in a continuous bubble column reactor operated with 35 %v•v^{-1} CH_4 and 6 % ww^{-1} NaCl at 20 ºC. Likewise, [10] achieved a maximum ectoine content of 105.0 ± 27.2 mg·g biomass^{-1} and a hydroxyectoine content of 24.2 ± 5.4 mg·g biomass^{-1} with a methanotrophic consortium in fed-batch stirred tank reactors after four feeding cycles with an initial CH_4 concentration of 9 %v•v^{-1} in the headspace, a NaCl concentration of 6 %w•w^{-1} and a temperature of 15 ºC.

Unfortunately, CH_4 is a hydrophobic gas with a low Henry's law constant (H=gas concentration/liquid concentration=30 at 25 °C), and its aqueous solubility decreases as the concentration of NaCl increases [11,12]. Maximum CH_4 bioconversion efficiencies up to 57 % and 70 % have been previously reported in stirred tank bioreactors without and with silicone oil, respectively [13,14]. Likewise, CH_4 bioconversion efficiencies ranging from 25 % to 66 % have been achieved in bubble column bioreactors with internal gas recirculation [6,15]. In this context, the low CH_4 gas-liquid mass transfer is a critical limitation for the development of innovative biogas biorefineries [16].

Taylor flow bioreactors can contribute to overcoming gas-liquid mass transfer limitations since their mass transfer coefficients are one order of magnitude higher than those of other turbulent gas-phase bioreactors under the same energy inputs [17,18]. Taylor Flow reactors consist of capillaries between 1 and 5 mm in diameter where Taylor flow occurs [18]. This flow regime is based on a train of co-current gas bubbles and liquid slugs that enhances mass transfer through internal fluid recirculation and the high specific area [18,19]. Despite the potential of Taylor Flow bioreactors for CH_4 bioconversion, the optimization of the key design and operational parameters has not been systematically carried out to date.

In this work, the influence of the gas residence time (GRT), internal gas recirculation flow rate ($Q_g$rec), liquid recirculation flow rate (Q_l) and capillary tube length on CH_4 bioconversion and ectoines production was evaluated in a novel multicapillary Taylor flow bioreactor using a mixed methanotrophic culture under high salinity conditions.

2. Materials and methods

2.1. Inoculum, mineral salt medium and gas feeding

The inoculum used in the Taylor flow bioreactor was a consortium of halophilic methanotrophic bacteria used in earlier experiments in the laboratories of the Institute of Sustainable Processes (Valladolid, Spain), which was stored at 4 °C prior to inoculation. The pre-inoculum was enriched from a salt lagoon (Poza de Sal, Spain) by [10] and exhibited a high ectoine and hydroxyectoine production potential. The mineral salt medium (MSM) used in all the experiments in the Taylor flow reactor contained 6 %w•w^{-1} NaCl and the following chemicals (g•L^{-1}): 0.1088 KH_2PO_4, 0.125 $Na_2HPO_4 \cdot 2\ H_2O$, 3.78 $NaHCO_3$, 0.53 Na_2CO_3, 0.2 $MgSO_4 \cdot 7\ H_2O$, 0.013 $CaCl_2 \cdot 2\ H_2O$, 3 KNO_3, 26 µL of $Na_2WO_2 \cdot 2\ H_2O$ solution (2.7 g•L^{-1}) and 2 mL of the same trace elements used in [10].

Methane was fed from a cylinder with a purity of 99.5 %v•v^{-1} (Carburos Metálicos S.A., Spain), whereas pre-treated air (after impurities removal with an activated carbon filter and a dehumidifier) was supplied by a compressor (SMART 18, SCC, Spain).

2.2. Experimental set-up

The experimental work was carried out in a Taylor flow reactor with a total volume of 9.3 L and 25 capillary glass tubes, through which the liquid and gas phases circulated co-currently upwards from a 2.5 L polyvinyl chloride (PVC) chamber up to a 6.5 L PVC chamber (Fig. 1). The capillaries had an internal diameter of 3 mm and a length of 1.50 m or 0.75 m, depending on the operational stage. The working volume in the reactor was 5.6 L and 5.2 L when operated with 1.50 m and 0.75 m capillaries, respectively. The culture broth, *i.e.* the methanotrophic consortium suspended in the MSM, was mechanically recirculated via a centrifugal pump (Oase, EDEN 159) from the upper to the lower module. A liquid extraction basket installed in the middle section of the vessel facilitated its separation from the gas phase in the upper chamber. This prevented the entrance of gas bubbles in the liquid recirculation stream. The gas outlet located at the top of the upper module, allowed the discharge of one fraction of the CH_4-depleted gas mixture into the atmosphere, while the remaining portion was recirculated. The recirculated gas, regulated by a rotameter (Aalborg, Germany), was conducted to a water trap to eliminate foams and water drops, and then directed to a gas compressor (H5P3 EAD, Spain) coupled with a condenser to

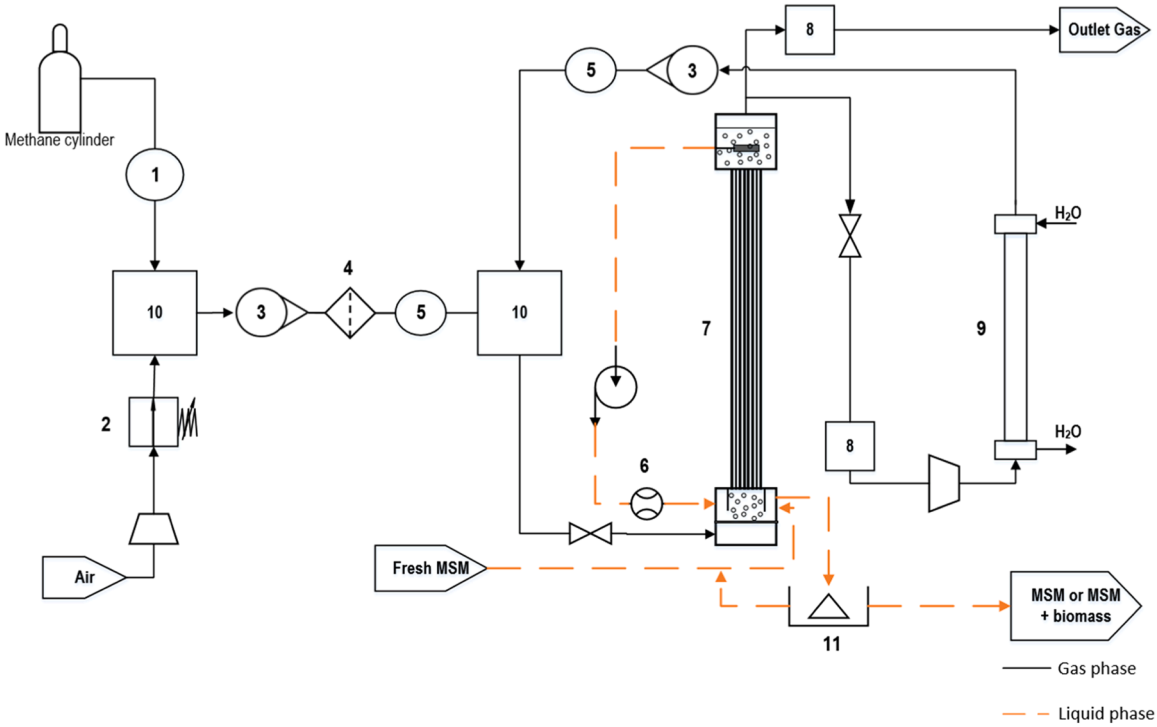

Fig. 1. Experimental system comprising (1) Mass flow controller, (2) Pressure controller, (3) Rotameter, (4) Gas filter (0.22 μm), (5) Sampling port, (6) Liquid flow meter, (7) Taylor flow reactor, (8) Water trap, (9) Condenser, (10) Gas mixing chamber, (11) Centrifuge.

effectively remove humidity. Finally, it was mixed with the inlet gas stream.

The inlet CH_4 stream from the cylinder and the pre-treated air stream were mixed in a 0.94 L PVC mixing chamber. The resulting mixture was filtered through a 0.22 μm cellulose acetate filter to remove dust and microorganisms before being combined with the recirculated gas in a second 3.15 L PVC mixing chamber. Flow rates were controlled to ensure an inlet methane concentration $\leq$5 %v•v^{-1}. Gas sampling ports were installed after the first mixing chamber and in the recirculation gas line to measure the gas composition for the subsequent calculation of CH_4 removal and CO_2 production.

The mixture of air-methane inlet and recirculation gas was injected into the lower chamber. Within this chamber, a neoprene membrane with a pore size of 0.5 mm ensured the homogeneous sparging of the gas into the liquid media recirculated from the upper module. A pressure controller installed in the air line ensured an overpressure of ~0.8 bar, guaranteeing that the gas flow overcame the pressure drop of the membrane and the water column. Gas and liquid flow rates were controlled to guarantee that both phases moved through the capillary tubes to the upper chamber with a Taylor-flow hydrodynamic pattern. Liquid flow rates were measured with a flow meter (Fischer & Porter Iberica, 10A1197A) before re-entering the bottom module of the reactor.

Taylor flow is a segmented flow pattern of liquid slugs and gas bubbles surrounded by a thin film of liquid [20,21]. Taylor flow occurs within the capillaries of the reactor (Figure S4, supplementary material) under certain operational conditions. This flow pattern improves liquid-gas matter transfer and reduces the energy required in the system due to the dominance of capillary forces over gravity and viscosity [21].

2.3. Experimental design

The experimental design, summarized in Table 1, aimed at evaluating the influence of $Q_g$rec, Q_l, GRT and capillary length on CH_4 consumption, CO_2 production and ectoines accumulation by the methanotrophic consortia. The experiments were conducted in three test series. During Test Series A, the liquid recirculation flow rate was set at 395 L•h^{-1}, whereas gas recirculation flow rates of 1.0 L•min^{-1}, 2.5 L•min^{-1}, 4.0 L•min^{-1}, and 5.5 L•min^{-1} were assessed under GRTs of 60 and 120 min using 1.50 m capillaries. In Test Series B, liquid recirculation flow rates of 141 L·h^{-1}, 165 L·h^{-1}, 395 L·h^{-1} and 434 L·h^{-1} were assessed under a GRT of 60 min and a gas recirculation flow rate of 5.5 L·min^{-1} using 1.50 m capillaries. Test Series C was carried out under the same operational conditions as Test Series B but with capillary tube lengths of 0.75 m instead of 1.50 m, which entailed a decrease in the working volume of the bioreactor from 5.6 L to 5.2 L.

Table 1
Operational conditions of the experiments performed in the Taylor Flow Bioreactor. Q_l: liquid recirculation flow, $Q_g$rec: gas recirculation flow, GRT: gas residence time, Lc: capillary length.

Test Series	Stage	Elapsed Time (days)	Q_l (L·h^{-1})	$Q_g$rec (L·min^{-1})	GRT (min)	Lc (m)
A	I	45	395	1.0	120	1.50
	II			2.5		
	III			4.0		
	IV			5.5		
	V			1.0	60	
	VI			2.5		
	VII			4.0		
	VIII			5.5		
B	I	20	141	5.5	60	1.50
	II		165			
	III		395			
	IV		434			
C	I	17	0			0.75
	II		165			
	III		395			
	IV		434			

The $Q_g$rec and Ql ranges selected in this study corresponded to air and liquid velocities where the flow regime changed from bubble flow to Taylor flow in the 25 capillary set-up. The reference for the GRT herein tested were obtained from literature studies assessing methane

treatment in bioreactors. The capillary lenght of 1.5 m was the standard length of commercial glass capillaries, and was selected to decrease the investment costs.

The inlet and outlet gas streams and the cultivation broth were analysed three days per week in Test Series A, increasing the gas phase sampling frequency to five days per week in Test Series B and C.

The biomass concentration in the culture broth was measured in terms of total suspended solids (TSS) and was adjusted to 1.0–1.5 $gTSS \bullet L^{-1}$ throughout the entire experimental period. An aliquot of 10 % $v \bullet v^{-1}$(560 mL or 520 mL) of the culture broth was removed and replaced with fresh MSM on a daily basis. When biomass removal was not required, the culture was centrifuged (4200 rpm × 7 min) and the pellet was resuspended in fresh MSM. When biomass removal was needed to maintain a constant TSS concentration in the bioreactor, a fraction of the biomass withdrawn was discarded.

Gas samples of 100 μL were taken in duplicate from the inlet and recirculation gas streams using gas-tight syringes to measure the concentration of CO_2 and CH_4. The flow rates of the inlet and outlet streams and the pressure of the inlet stream were also monitored to accurately calculate the bioconversion efficiency (CH_4-BE) and capacity (CH_4-BC) of CH_4. Liquid samples of 150 mL were taken to determine pH, conductivity, optical density (OD), TSS, dissolved total nitrogen (TN), dissolved total organic carbon (TOC), dissolved inorganic carbon (IC) and intracellular ectoine (EC) and hydroxyectoine (HE) concentrations. All analyses were carried out in technical duplicates. The remaining liquid sample after all measurements was returned to the bioreactor.

2.4. Analytical procedures

Gas composition was analysed in a Bruker 430 gas chromatograph (GC-TCD) (Palo Alto, USA) equipped with a thermal conductivity detector, and a CP-Molsieve 5 A and a CP-PoraBOND Q columns. The temperature of the injector, oven and detector were held constant for 5 min at 150, 45 and 200 ºC, respectively [9]. The pH and conductivity in the culture broth were measured with a Basic 20+ pH-meter (Düsseldorf, Germany) and an EC-Meter BASIC 30 instrument (Barcelona, Spain), respectively. The OD was quantified with a spectrophotometer Shimadzu UV-2550 UV/Vis (Shimadzu, Japan). Biomass concentration as TSS was measured using a modification of the standard method [22]. Because of the thermal sensitivity of the filter material (mixed cellulose esters), the filtered biomass sample could only be dried at 105℃ for 24 h to determine TSS. However, the analysis of volatile suspended solids was not feasible due to the high temperatures (550 ºC) required. Thus, to ensure a reliable quantification of the biomass, the culture broth sample was centrifuged to remove the MSM, and the biomass pellet was resuspended in miliQ water. The sample was filtered through 0.45 μm pore size filters and additional water was rinsed to assure the complete removal of salt from the filter. Additionally, dissolved TN, TOC and IC concentrations were determined after filtration of the sample through a 0.45 μm pore size filter in a TOC-VCSH analyser (Japan) with a TNM-1 chemiluminescence module.

Inlet and outlet gas flow rates were double-checked by the water displacement method in a Test probe. A needle valve and a PN5007 Electronic pressure sensor (Ifm, Germany) were installed on the gas line during inlet flow rate measurements to replicate the overpressure experienced by the inlet gas pipeline during operation.

Intracellular EC and HE concentrations were quantified in duplicate using 2 mL of culture broth centrifuged at 9000×g for 10 min. The supernatant was discarded, 1.8 mL of miliQ water with 6 % $w \bullet w^{-1}$ NaCl was added, and the biomass was resuspended with a vortex mixer (Velp scientific ZX3, Italy). The samples were centrifuged again and the washing was repeated to remove MSM residuals that can eventually interfere HPLC determinations. An aliquot of 1.8 mL of ethanol 70 % $v \bullet v^{-1}$ and 25 ± 5 mg of 0.1 mm-diameter of zirconia/silica beads were added to the cell suspension to break the cells into a Mini-BeadBeater-16 (BioSpec, Spain) at 1048×g for 10 min. Then, the samples were centrifuged at 9000×g for 15 min and filtered through a 0.22 μm pore size filter. The analyses were conducted in HPLC-UV, as described by [10] in a HPLC-V 717 plus autosampler (Waters, Bellefonte, USA) coupled to an UV Dual λ Absorbance detector (Waters, Bellefonte, USA) operated at 220 nm and 40 °C. The columns used were a L8 Spherisorb Amino (NH_2) column (Waters, Spain) or Polaris 3 NH_2 column (Agilent, UE) and a C18 AQ + pre-column (Sigma Aldrich, Spain). The mobile phase consisted of a 75:25 acetonitrile:miliQ water mixture at a flow rate of 0.6 $mL \bullet min^{-1}$. External standards were prepared with commercial EC and HE (purity ≥ 95 %, Sigma Aldrich) diluted in ethanol 70 % $v \bullet v^{-1}$.

2.5. Calculations

Methane conversion by the methanotrophic consortium was calculated using the methane bioconversion efficiency (CH_4-BE) and CH_4 bioconversion capacity (CH_4-BC) as a proxy. These parameters were calculated using Eqs. 1 and 2, and the volumetric CO_2 production (PCO_2) was estimated using Eq. 3:

$$CH_4 - BE(\%v \bullet v^{-1} \quad CH_4) = \frac{\dot{m}_{CH4,IN} - \dot{m}_{CH4,OUT}}{\dot{m}_{CH4,IN}} \times 100 \tag{1}$$

$$CH_4 - BC(g \quad CH_4 \bullet m^{-3} \bullet h^{-1}) = \frac{\dot{m}_{CH4,IN} - \dot{m}_{CH4,OUT}}{V_{reactor}} \tag{2}$$

$$PCO_2 \quad (g \quad CO_2 \bullet m^{-3} \bullet h^{-1}) = \frac{\dot{m}_{CO2,OUT} - \dot{m}_{CO2,IN}}{V_{reactor}} + \frac{Q_{L,MS} \quad * \quad (IC_{L,OUT} - IC_{L,IN})}{V_{reactor}} \times \frac{MW_{CO2}}{MW_C} \tag{3}$$

where, $\dot{m}_{CH_4,IN}$ and $\dot{m}_{CH4,OUT}$ are the inlet and outlet mass flow rates of methane gas (g $CH_4 \bullet h^{-1}$) and $V_{reactor}$ the reactor liquid volume (m^3). Similarly, $\dot{m}_{CO2,IN}$ and $\dot{m}_{CO2,OUT}$ are the inlet and outlet mass flow rates of carbon dioxide gas (g $CO_2 \bullet h^{-1}$) and $Q_{L,MSM}$ the fresh MSM exchange flow rate (0.021 $L \bullet h^{-1}$). $IC_{L,IN}$ and $IC_{L,OUT}$ correspond to the inorganic carbon concentrations (g $C \bullet L^{-1}$) in the fresh MSM and in the culture broth, respectively, while MW_{CO2} and MW_C stand for the molecular mass of carbon dioxide and carbon.

Liquid (v_{liquid}) and gas (v_{gas}) velocities per capillary were calculated following Eq. 4 and Eq. 5.

$$v_{liquid} = \frac{Q_{liquid\ reactor}}{n_c * A_{capillary}} \tag{4}$$

$$v_{gas} = \frac{Q_{gas\ reactor}}{n_c * A_{capillary}} \tag{5}$$

Where $Q_{liquid\ reactor}$ and $Q_{gas\ reactor}$ are the total liquid and gas flow rate that enter in the Taylor flow bioreactor. N_c is the number of capillaries in the reactor (25 tubes) and $A_{capillary}$ is the area of each capillary considering a diameter of 3 mm.

2.6. Bacterial community analysis

Bacterial community analysis was performed for both the inoculum and the samples withdrawn at steady state at the end of each *Test Series*. Aliquots of culture broth were centrifuged at 13,000×g. Approximately 200 mg of wet pellet were used for DNA extraction using the PowerSoil Pro kit (Qiagen, Germany) according to the manufacturer's instruction. The final DNA concentrations were measured using a Qubit 4 Fluorometer (Thermo Fisher Scientific, USA) and Qubit 1X dsDNA HS reagents. DNA extracts were sent to Novogene (UK) for Next Generation Sequencing (structure and composition of the microbial communities) of 16S rRNA genes of distinct regions (16SV4/16SV3/16SV3- V4/16SV4-V5, 18SV4/18SV9, ITS1/ITS2, ArcV4) on Illumina platform. Quality

control was done between each step of the procedure to maintain the reliability and accuracy of the data. Amplification was carried out by PCR, ligated with Illumina adapters and sequenced on the Illumina paired-end platform. The bioinformatics analysis pipeline included data split, sequence assembly (FLASH V1.2. 1 1), data filtration (Fastp V0.23.1), analysis using the Silva database and quimera removal (vsearch package V2 16.0). Denoise was performed with DADA2 or deblurmodule in the QIIME2 software (Version QIIME2–202202) to obtain initial ASVs (Amplicon Sequence Variants). Species annotation was performed using QIIME2 software. The sequences obtained were deposited in Genbank as PRJNA1108639.

2.7. Data treatment

The results for each parameter are reported as the average ± standard deviation of steady-state measurements calculated for each operational stage.

3. Results

3.1. Influence of the internal gas recirculation rate and GRT

During Test Series A, higher CH_4-BEs were achieved with the increase in $Q_g$rec flow rates (Fig. 2A). Maximum values of 83.8 ± 2.7 % and 71.4 ± 2.0 % were achieved at a $Q_g$rec flow rate of 5.5 L·min^{-1} under operation at a GRT of 120 and 60 min, respectively. At 60 min of GRT, the increase in $Q_g$rec to 5.5 L•min^{-1} enhanced the bioconversion capacity and CO_2 production up to 25.4 ± 1.9 g CH_4•m^{-3}•h^{-1} and 42.5 ± 2.1 g CO_2•m^{-3}•h^{-1}, respectively (Figs. 2B and 2C). Constant values of CH_4-BC and PCO_2 were achieved during operation at GRTs of 120 min at $Q_g$rec flow rates between 2.5 and 5.5 L•min^{-1}. In addition, CH_4-BE was very similar at 120 min of GRT at $Q_g$rec of 4.0 and 5.5 L·min^{-1}. The CO_2 production yield (Y_{CO2} = PCO_2/CH_4-BC) ranged from 1.10 to 2.07 g CO_2•g CH_4^{-1} during Test Series A.

Biomass concentration increased from an initial value of 0.38 ± 0.01 gTSS•L^{-1} until day 44 of operation. Afterwards, TSS concentration was adjusted to ~1 g•L^{-1} by periodic biomass wasting. TN consumption due to biomass and osmolyte production was compensate by addition of MSM and always kept above 109 mg N•L^{-1}. TOC concentrations remained below 122 mg C•L^{-1}, indicating no major cell lysis or decay during Test Series A. pH and conductivity remained at 8.25 ± 0.08 and 83.4 ± 4.5 mS•cm^{-1}, typical values for halotolerant methanotrophic bacteria (Table S1 in supplementary material) [3,7,23].

The EC content (Fig. 3A) increased with the increase in $Q_g$rec from 1.0 to 4.0 L•min^{-1}, remaining relatively constant at higher $Q_g$rec values. Maximum values of 105.1 ± 8.6 mg_{EC}·g_{TSS}^{-1} at 4.0 L•min^{-1} and 120 min GRT and of 107.5 ± 40.3 mg_{EC}·g_{TSS}^{-1} at 2.5 L•min^{-1} and 60 min GRT were recorded. The HE content (Figure S5A, supplementary material) exhibited a similar behaviour, reaching 26.0 ± 3.2 mg_{HE}·g_{TSS}^{-1} at 4.0 L•min^{-1} and 120 min of GRT, and 33.4 ± 11.7 mg_{HE}·g_{TSS}^{-1} at 2.5 L•min^{-1} and 60 min GRT.

3.2. Influence of liquid recirculation rate and capillary length

During Test Series B, CH_4 bioconversion increased at higher Q_l values, as evidenced by the higher CH_4-BE of 77.4 ± 0.1 % and CH_4-BC of 25.9 ± 0.6 g CH_4•m^{-3}•h^{-1} recorded at a Q_l of 434 L•h^{-1} with a capillary length of 1.5 m (Figs. 4A and 4B). Operation at a shorter capillary length of 0.75 m (Test Series C) resulted in lower methane bioconversion rates. PCO_2 increased with the increase in recirculation flow rates, with higher CO_2 production at Q_l ranging from 165 to 434 L h^{-1} (Fig. 4C). Interestingly, CO_2 production reached a slightly higher value of 49.5 ± 2.0 g CO_2•m^{-3}•h^{-1} at 434 L•h^{-1} with a capillary length of 0.75 m compared to 1.5 m. Increased CO_2 production in Test Series C might be due to variations in the microbial community structure, with CO_2-producing genera such as *Clostridium*, *Enterococcus* and *Rhodococcus* being dominant at a short capillary length [24–26]. In addition, a lower methane mass transfer might result in a higher methane carbon distribution towards energy production and cell maintenance (fostering CH_4 conversion to CO_2), rather than towards biomass and osmolyte production. The mineralization ratios achieved ranged between 1.25 and 2.17 g CO_2•g CH_4^{-1}.

The biomass concentration was adjusted by periodic wasting in order to maintain an average value of 1.8 ± 0.3 gTSS•L^{-1} and 1.41 ± 0.36 gTSS•L^{-1} during Test Series B and C, respectively. A maximum TOC concentration of 104 ± 2 mg C•L^{-1} and 27 mg C•L^{-1} was recorded with a capillary length of 1.5 m and 0.75 m, respectively. However, TN concentration decreased from 286 to 157 mg N•L^{-1} with increasing Q_l at a capillary length of 1.5 m, and remained constant at ~ 182 ± 35 mg N•L^{-1} with a capillary length of 0.75 m. In addition, the pH remained in the typical range for methanotrophic growth during Test Series B and C (8.3 ± 0.1) [3,7,23]. Likewise, conductivity remained constant at 84.7± 2.5 and 85.1 ± 2.5 in Test Series B and C, respectively (Table S2 and S3 in supplementary material) [7].

The ectoines content during Test Series B remained relatively constant, with average values of 25.4 ± 1.8 mg_{EC}·g_{TSS}^{-1} and 6.3 ± 0.5 mg_{HE}·g_{TSS}^{-1} (Fig. 3B and Figure S5B). When the Taylor Flow reactor was operated at a capillary length of 0.75 m (Test Series C), higher contents of ectoines (38.8 ± 6.9 mg_{EC}·g_{TSS}^{-1} and 9.7 ± 2.7 mg_{HE}·g_{TSS}^{-1}) were recorded at a Q_l of 0 L•h^{-1}, subsequently decreasing at higher flow rates.

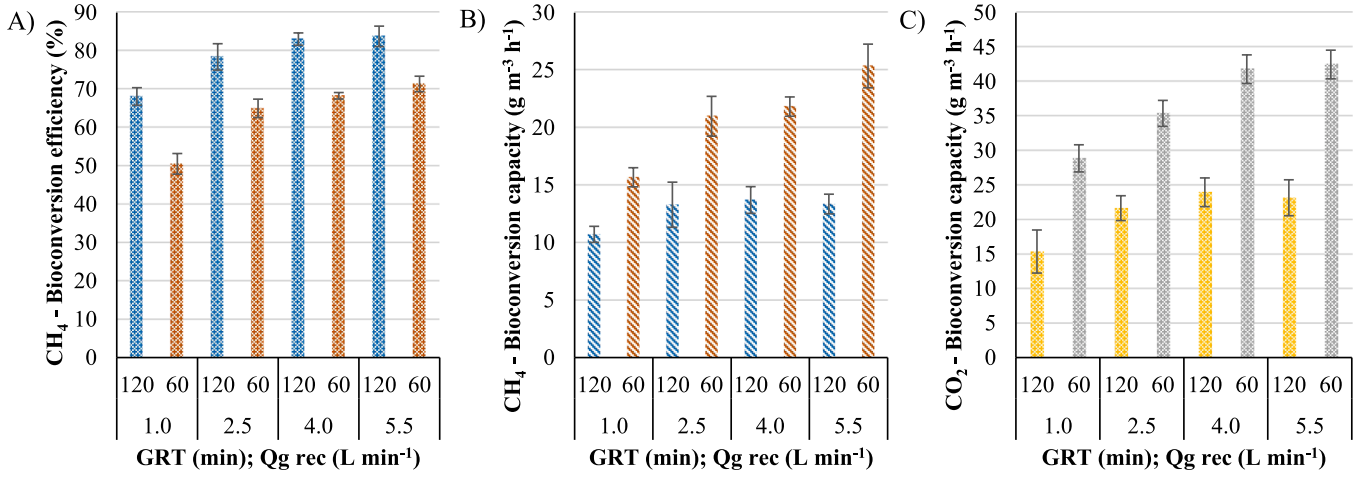

Fig. 2. Influence of Q_{grec} and GRT on methane bioconversion efficiency (A), methane bioconversion capacity (B) and total CO_2 production (C).

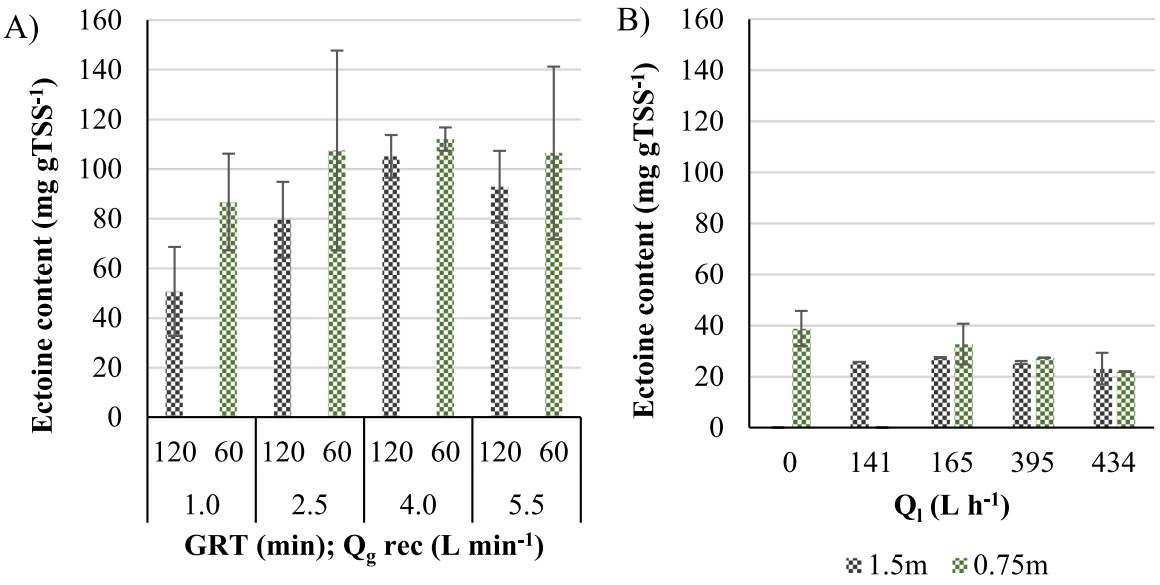

Fig. 3. Influence of $Q_g$rec and GRT (A) and Q_l and Lc (B) on ectoine intracellular content.

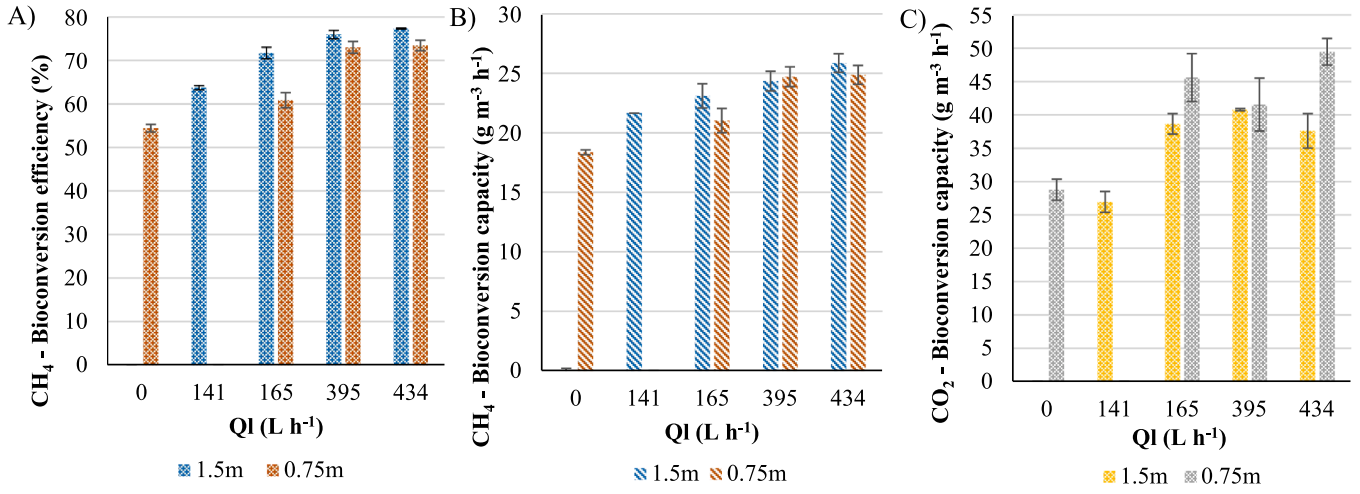

Fig. 4. Influence of Q_l and Lc on methane bioconversion efficiency (A), methane bioconversion capacity (B) and total CO_2 production (C) in Taylor Flow reactors constructed with capillary tubes lengths of 1.5 m and 0.75 m.

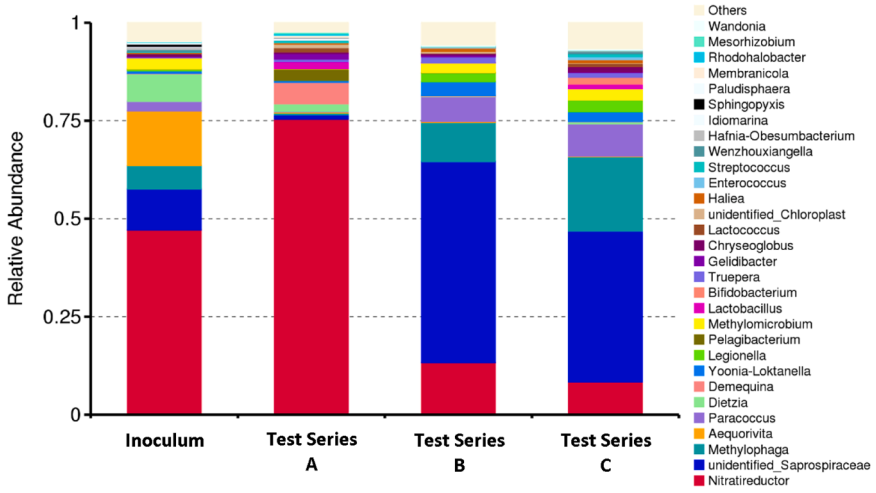

Fig. 5. Taxonomic diversity at a genus level of the inoculum and of the cultures prevailing at the end of Test Series A, B and C.

3.3. Microbial communities in the methanotrophic consortia

The microbial community inoculated in the Taylor Flow reactor was dominated by Proteobacteria (65.1 %), Bacteroidota (25.2 %) and Actinobacteriota (8.3 %). During Test Series A, the dominant phyla were Proteobacteria (81.8 %), which comprised mainly the classes Alpha- (97.7 %) and Gamma- (2.3 %) proteobacteria, Actinobacteriota (8.5 %), Bacteroidota (4.2 %) and Firmicutes (3.8 %). In Test Series B, Proteobacteria population decreased to 42.2 % (61.1 % Alpha and 38.9 % Gammaproteobacteria), whereas Bacteroidota increased to 52.8 % and Actinobacteriota and Deinococcota exhibited dominances of 1.5 %. During Test Series C, Proteobacteria decreased to 49.6 % (44.4 % alpha and 55.6 % gammaproteobacteria), Bacteroidota showed a dominance of 39.6 %, Actinobacteriota 4.7 %, Firmicutes 4.0 % and Deinococcota 1.2 %.

At the genus level (Fig. 5), the inoculum was dominated by *Nitratireductor* (47.1 %), unidentified_*Saprospiraceae* (10.5 %), *Methylophaga* (6.0 %), *Aequorivita* (13.9 %), *Paracoccus* (2.4 %) and *Dietzia* (7.0 %). At the end of Test Series A, the consortium was dominated mainly by *Nitratireductor* (75.4 %), with a lower presence of unidentified_*Saprospiraceae* (1.1 %), *Dietzia* (1.9 %), *Demequina* (5.5 %), *Pelagibacterium* (2.9 %) and *Lactobacillus* (1.8 %). At the end of Test Series B, the dominant genus shifted to unidentified_*Saprospiraceae* (51.3 %), followed by *Nitratireductor* (13.3 %), *Methylophaga* (10.0 %), *Paracoccus* (6.4 %), *Yoonia-Loktanella* (3.5 %), *Legionella* (2.3 %), *Methylomicrobium* (2.5 %) and *Truepera* (1.5 %). Similar to Test Series B, during Test Series C unidentified_*Saprospiraceae* (38.5 %) was the dominant genus, followed by *Nitratireductor* (8.4 %), *Methylophaga* (19.0 %), *Paracoccus* (8.3 %), *Yoonia-Loktanella* (2.5 %), *Legionella* (2.9 %), *Methylomicrobium* (2.9 %), *Lactobacillus* (1.2 %), *Bifidobacterium* (1.7 %) and *Truepera* (1.5 %).

4. Discussion

4.1. CH_4 bioconversion and total CO_2 production

In Test Series A, CH_4-BE and CH_4-BC increased with the increase in $Q_g$rec, likely due to the higher velocities of the gas-liquid slugs, turbulence and a more homogeneous distribution of the gas-liquid mixture at the bottom of the reactor imposed by the increasing gas recycling. In addition, a higher $Q_g$rec entails a higher gas hold-up in the bioreactor and therefore higher methane mass transfer rates. During this test, Taylor flow prevailed in the multicapillary unit since the liquid velocity per capillary tube was 0.62 m•s^{-1} and the gas velocities ranged between 0.10 and 0.52 m•s^{-1}, which corresponded to the Taylor flow region determined by [19] in the same bioreactor (Fig. 6). The G/L velocities ratio was also in the optimum range of 0.16–0.85 regardless of the GRT [19]. Along with $Q_g$rec, the results achieved during Test Series B highlight the significant influence of increasing Q_l as an effective strategy to enhance the bioconversion of CH_4. On the other hand, operation with a shorter capillary length (Test Series C) resulted in lower methane bioconversion rates likely due to insufficient capillary length for a complete mass transfer of methane from the gas to the liquid phase. The length of the capillaries did not influence neither the gas-liquid distribution at the bottom module (which was determined by the number of capillaries and the gas-liquid turbulence) nor the establishment of a Taylor flow regime inside the capillary. The highest CH_4-BC recorded during the evaluation of the liquid recirculation rate and capillary length were found at liquid velocities of 0.68 m•s^{-1} and the lowest G/L velocity ratios (0.77), when Taylor flow occurred as observed by [19]. On the contrary, the lowest CH_4-BC were obtained under liquid velocities of 0.22 m•s^{-1} and, consequently, at the highest G/L velocity ratios.

Compared with process operation at a GRT of 120 min, operation at 60 min entailed lower methane conversion efficiencies in all experiments but resulted in higher bioconversion capacities, indicating that the microbial consortium could assimilate the higher methane loads fed to the reactor during operation at lower GRT. Regardless of the GRT, the CH_4 bioconversion was associated with its catabolism into CO_2 by the methanotrophic consortium [3]. Indeed, the CO_2 production yields ($Y_{CO2} = PCO_2/CH_4$-BC), which ranged from 1.10 to 2.07 g CO_2•g CH_4^{-1}, agreed with the typical values reported in the literature for methanotrophic consortia (0.7–2.5) [7,27–30]. Nevertheless, slightly higher CO_2 productions than the stoichiometric values corresponding to the methanotrophic CH_4 bioconversion were observed in all tests, likely due to the occurrence of metabolic processes producing CO_2 from substrates other than methane such as endogenous metabolism or the aerobic oxidation of extracellular metabolites [7].

Compared to previous studies using methanotrophic consortia, the CH_4 removal efficiencies herein achieved were notably high. [13] achieved removal efficiencies of 57–70 % by adding silicone oil in stirred tank bioreactors operated at high stirring rates (200–800 rpm). Similarly, [7] achieved maximum CH_4 removal efficiencies and bioconversions of 66 ± 2 % and 22 ± 21 g $CH_4 \cdot m^{-3} \cdot h^{-1}$ with a methanotrophic consortium in a 10 L bubble column bioreactor, with an inlet CH_4 concentration of 5 %v•v^{-1}, 3 %w•w^{-1} NaCl in the mineral medium and 43.5 min of GRT. Lower PCO_2 values (12.3–27.4 g $CO_2 \cdot m^{-3} \bullet h^{-1}$) were reported by [7] due to the lower CH_4-BC even working for higher CH_4 inlet flow rates. However, [13] observed a maximum PCO_2 of 75 ± 5 g $CO_2 \cdot m^{-3} \bullet h^{-1}$ due to the higher CH_4-BC (48 ± 4 g $CH_4 \cdot m^{-3} \bullet h^{-1}$) mediated by the addition of silicone oil. In this

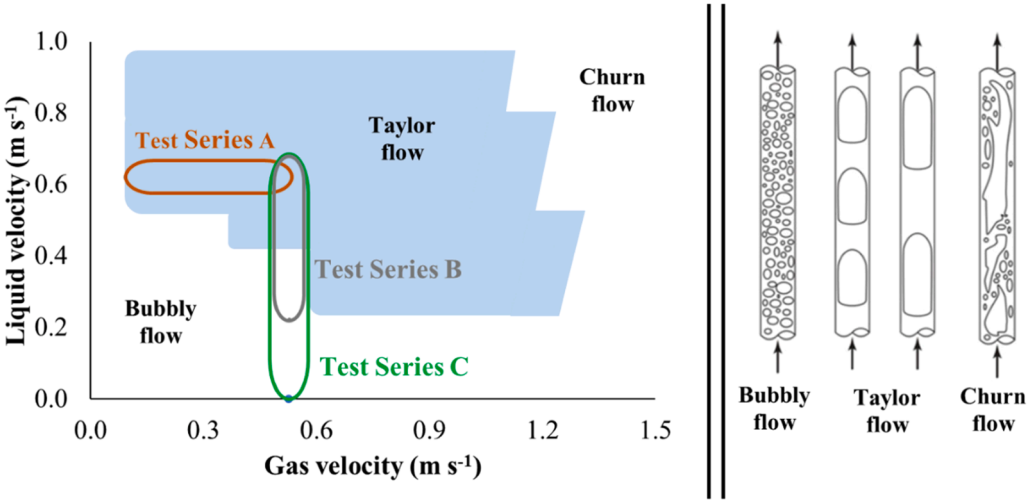

Fig. 6. Graph of flow distribution in capillaries according to gas and liquid velocity per capillary. Representation of the bubbling, Taylor and churn flow [19,20].

context, [15] obtained the highest CH_4-BC (73.8 ± 2.1 g CH_4•m^{-3}•h^{-1}) with a bubble column bioreactor under low (30 min) GRT due to the consistently higher inlet loads of 202 g CH_4•m^{-3}•h^{-1} compared to those of 73.8 ± 2.1 g CH_4•m^{-3}•h^{-1} tested in this study. However, at a GRT of 120 min and a recirculation ratio ($Q_g$rec•Q_{inlet}^{-1}) of 30, the CH_4-BE achieved by [15] was 39.0 ± 3.6 %. These lower efficiencies and bioconversions were probably associated to the lower gas-liquid transfer rates of bubble column bioreactors compared to Taylor flow reactors [17,18], reinforcing the potential of this bioreactor configuration for residual gas valorisation.

A previous experiment in our lab conducted in a 6 L Taylor flow reactor operating with a mixed methanotrophic culture capable of accumulating biopolymers, reached a CH_4-BE of 71.3 ± 1.4 % when working at 4 %v•v^{-1} of inlet CH_4 concentration, 60 min of GRT, $Q_g$rec of 3.5 L·min^{-1} and Q_l of 420 L·h^{-1} [19]. However, the maximum value of CH_4-BE hereby achieved (83.8 ± 2.7 %) was higher than the maximum CH_4 conversion efficiency reported by [19]. The PCO_2 was similar in both studies, with most values ranging between 25 and 50 g CO_2•m^{-3}•h^{-1} under process operation at GRTs of 60 min.

4.2. Ectoine and hydroxyectoine content

The results achieved suggested that higher methane bioconversions induced higher ectoine and hydroxyectoine biosynthesis. This increasing production of osmolytes with higher methane bioconversion rates was also reported in previous experiments [14]. In addition, the osmolite-specific production was consistently higher for ectoine than for hydroxyectoine, regardless of the GRT and $Q_g$rec, likely due to the higher presence of ectoine-producing bacteria (for example *Nitratireductor*, *Methylophaga* and *Methylomicrobium*) as seen in previous experiments with a similar consortium [7,10]. In addition, the ectoines intracellular content was considerably higher in Test Series A than in Test Series B and C, likely due to the shift in the dominant microorganisms in the methanotrophic consortium. However, significantly higher TSS concentrations were also observed by the end of Test Series B compared to Test Series A, which caused a decrease in the ectoines content as reported by [7] as a result of the lower specific methane uptake. [23] and [31], after several batch trials with the strain *Methylobacter alcaliphilus 20Z,* achieved one of the highest methanotrophic ectoine contents of 145.2 mg_{EC}·g_{TSS}^{-1}, under a CH_4:air ratio of 1:1 in a MSM with 6 % w•w^{-1} NaCl. The higher CH_4 concentration in the gas phase was likely the main reason for the higher ectoine content observed in this work. However, *M. marinus* and *M. kenyense* exhibited lower ectoine contents (60–70 mg_{EC}·g_{TSS}^{-1}) than the specific concentrations herein recorded during Test Series A [32].

Similar ectoine contents (105.0 ± 27.2 mg_{EC}·g_{TSS}^{-1} and 24.2 ± 5.4 mg_{HE}·g_{TSS}^{-1}) were observed in a similar halophilic microbial consortium by [10], who used 1.2 L fed-batch bioreactors under a CH_4 headspace of 9 %v•v^{-1} (replaced four times) at 6 %w•w^{-1} NaCl. In addition, [9] observed an ectoine content of 108.7 ± 4.8 mg_{EC}·g_{TSS}^{-1} with a mixed halophilic consortium grown in a 2 L bubble column reactor, under 35 % v•v^{-1} CH_4 and 6 %w•w^{-1} NaCl. The ectoine and hydroxyectoine contents reported by [9] were similar to those recorded in Test Series A, despite the higher concentration of CH_4 fed compared to the 5 % v•v^{-1} CH_4 in this work. Finally, [7] observed 47 ± 3 mg_{EC}·g_{TSS}^{-1} and 7 ± 0 mg_{HE}·g_{TSS}^{-1} in a similar methanotrophic consortium cultivated in a 10 L bubble column bioreactor under 5 %v•v^{-1} CH_4, 6 %w•w^{-1} NaCl and 25 ºC, values within the same range as those achieved during Test Series B and C.

4.3. Microbial population structure

The presence of ectoine producers among the microbial consortium was a key parameter governing ectoines accumulation. Some phyla such as Proteobacteria, Bacteroidota, and Actinobacteriota were also identified in mixed methanotrophic cultures able to generate ectoine [10], while many methanotrophic bacteria belonged to Gammaproteobacteria and Alphaproteobacteria classes and are capable of fixing carbon from methane via the RuMP or Serine cycle, respectively [3,33]. In this study, the dominance of genera such as *Nitratireductor* and *Aequorivita* agreed with previous works carried out with the same pre-inoculum under a NaCl concentration of 6 %w•w^{-1} [7]. Indeed, the dominance of *Nitratireductor* was the main characteristic of Test Series A, corresponding with the higher intracellular ectoines accumulation. In this sense, high shares of *Nitratireductor* seemed to enhance the production of ectoine and hydroxyectoine. This genus has been previously identified in methane to ectoine bioconversion experiments. It possess the ability to synthesise ectoine under salt stress conditions, utilizing nitrate as an electron donor and sugars and amino acids as carbon source [7,9].

During Test Series B and C, a more diverse microbial community was likely favoured by the increases in Q_l flow rates, where an *unidentified_Saprospiraceae* exhibited relatively higher shares. This genus belongs to the Saprospiraceae family, with previous studies suggesting the ability of members of this family to synthesise different osmoprotectant substances in saline media such as trehalose, proline, choline and betaine [34]. In this context, the shift from *Nitratireductor* in Test Series A to *unidentified_Saprospiraceae* in Tests Series B and C could have resulted in the accumulation of other osmoprotectant different than ectoine and hydroxyectoine.

Other genera with relevant dominance during Test Series B and C, such as *Methylomicrobium* and *Methylophaga* were also reported in halotolerant methanotrophic consortia as methane and methanol oxidizers and ectoine producers [9,35,36]. Although [9] concluded that a consortium with *Halomonas*, *Marinobacter*, *Methylophaga* and *Methylomicrobium* improved the bioconversion of biogas to ectoine, the increases in *Methylophaga* and *Methylomicrobium* dominances in our particular test did not trigger ectoine production during Test Series B and C. This is probably due to differences in the culture composition and interactions within the consortium, which impact on the content of ectoine that each bacteria can accumulate. Another possible consumer of methane or methanol was *Paracoccus* due to its capability of degrading various C1 compounds [37]. Finally, the presence of other genera in lower shares, such as *Yoonia-Loktanella* was not surprising due to their capacity to adapt to highly saline environments, generating demethylation enzymes [38]. The contribution of low relative abundance microorganisms could be relevant as they play a key role in the global consortium, using intermediates of methane oxidation metabolism as energy or carbon source [10].

5. Conclusion

This study optimized the gas and liquid recirculation flow rate and capillary length in a Taylor flow multicapillary reactor to improve methane bioconversion and ectoines synthesis. Higher gas and liquid recirculation flow rates under velocities that ensured Taylor flow improved methane bioconversion to efficiencies up to 84 %. High GRTs are recommended to enhance CH_4-BE albeit at the expense of lower CH_4-BCs. Nevertheless, the largest enhancement in CH_4-BCs from 13 to 25 g CH_4•m^{-3}•h^{-1} was achieved when $Q_g$rec was decreased from 120 to 60 min. A capillary length of 0.75 m resulted in lower methane conversions compared to capillaries of 1.5 m length. Higher methane transfer rates improved the synthesis of ectoine and hydroxyectoine by up to 71 %. *Nitratireductor* was the predominant genus in the period with maximum ectoines production, while *Methylomicrobium* and *Methylophaga* were likely the main responsible for methane consumption.

CRediT authorship contribution statement

Andrés Felipe Torres Franco: Writing – review & editing. **Wendy Mylene Llamas-Ramos:** Methodology, Investigation. **Víctor Monsalvo:** Writing – review & editing. **Patricia Zamora:** Writing – review & editing. **Raul Munoz:** Writing – review & editing, Validation,

Supervision, Resources, Funding acquisition, Formal analysis, Conceptualization. **Raquel Herrero-Lobo:** Writing – original draft, Methodology, Investigation, Formal analysis. **Frank Rogalla:** Writing – review & editing. **Raquel Lebrero:** Writing – review & editing, Validation, Supervision. **María del Rosario Rodero:** Writing – review & editing, Validation, Supervision.

Declaration of Competing Interest

The authors declare that they have no known competing financial interests or personal relationships that could have appeared to influence the work reported in this paper.

Data availability

Data will be made available on request.

Acknowledgements

This investigation was financed by CHEERS project. The project has been funded by the European Union's Horizon Europe Research and Innovation programme under Grant Agreement No 101060814. UK participants in Horizon Europe Project CHEERS are supported by UKRI grant numbers 10050977 Earthwatch Europe. The authors would like to thank the regional government of Castilla y León for the predoctoral contract of Raquel Herrero Lobo. María del Rosario Rodero acknowledges the NextGenerationEU Margarita Salas programme from the European Union for her research contract. The Regional Government of Castilla y León and the EU-FEDER programme (CL-EI-2021-07. UIC 315) are also gratefully acknowledged.

Appendix A. Supporting information

Supplementary data associated with this article can be found in the online version at doi:10.1016/j.jece.2024.114323.

References

[1] J. Becker, C. Wittmann, Microbial production of extremolytes — high-value active ingredients for nutrition, health care, and well-being, Curr. Opin. Biotechnol. 65 (2020) 118–128, https://doi.org/10.1016/J.COPBIO.2020.02.010.

[2] V. Pérez, J.L. Moltó, R. Lebrero, R. Muñoz, Ectoine production from biogas: a sensitivity analysis. Effect of local commodity prices, economy of scale, market trends and biotechnological limitations, J. Clean. Prod. 369 (2023) 133440, https://doi.org/10.1016/J.JCLEPRO.2022.133440.

[3] A. Gęsicka, P. Oleskowicz-Popiel, M. Łężyk, Recent trends in methane to bioproduct conversion by methanotrophs, Biotechnol. Adv. 53 (2021) 107861, https://doi.org/10.1016/J.BIOTECHADV.2021.107861.

[4] F. Orhan, E. Ceyran, A. Akincioğlu, Optimization of ectoine production from Nesterenkonia xinjiangensis and one-step ectoine purification, Bioresour. Technol. 371 (2023) 128646, https://doi.org/10.1016/J.BIORTECH.2023.128646.

[5] K. Hobmeier, M. Oppermann, N. Stasinski, A. Kremling, K. Pflüger-Grau, H. J. Kunte, A. Marin-Sanguino, Metabolic engineering of Halomonas elongata: ectoine secretion is increased by demand and supply driven approaches, Front. Microbiol. 13 (2022) 968983, https://doi.org/10.3389/FMICB.2022.968983/BIBTEX.

[6] M. del R. Rodero, A.A. Carmona-Martínez, C. Martínez-Fraile, R. Herrero-Lobo, E. Rodríguez, P.A. García-Encina, M. Peña, R. Muñoz, Ectoines production from biogas in pilot bubble column bioreactors and their subsequent extraction via biomilking, Water Res 245 (2023) 120665, https://doi.org/10.1016/J.WATRES.2023.120665.

[7] M. del R. Rodero, R. Herrero-Lobo, V. Pérez, R. Muñoz, Influence of operational conditions on the performance of biogas bioconversion into ectoines in pilot bubble column bioreactors, Bioresour. Technol. 358 (2022) 127398, https://doi.org/10.1016/J.BIORTECH.2022.127398.

[8] T. Badouard, D. Moreira De Oliveira, J. Yearwood, P. Torres, Final Report-Cost of Energy (LCOE) Study on energy costs, taxes and the impact of government interventions on investments in the energy sector, (2020). https://energy.ec.europa.eu/system/files/2020-10/final_report_levelised_costs_0.pdf (accessed September 24, 2023).

[9] S. Cantera, V. Phandanouvong-Lozano, C. Pascual, P.A. García-Encina, R. Lebrero, A. Hay, R. Muñoz, A systematic comparison of ectoine production from upgraded biogas using Methylomicrobium alcaliphilum and a mixed haloalkaliphilic consortium, Waste Manag 102 (2020) 773–781, https://doi.org/10.1016/J.WASMAN.2019.11.043.

[10] A.A. Carmona-Martínez, E. Marcos-Rodrigo, S. Bordel, D. Marín, R. Herrero-Lobo, P.A. García-Encina, R. Muñoz, Elucidating the key environmental parameters during the production of ectoines from biogas by mixed methanotrophic consortia, J. Environ. Manag. 298 (2021) 113462, https://doi.org/10.1016/J.JENVMAN.2021.113462.

[11] S. Cantera, R. Muñoz, R. Lebrero, J.C. López, Y. Rodríguez, P.A. García-Encina, Technologies for the bioconversion of methane into more valuable products, Curr. Opin. Biotechnol. 50 (2018) 128–135, https://doi.org/10.1016/J.COPBIO.2017.12.021.

[12] Z. Duan, S. Mao, A thermodynamic model for calculating methane solubility, density and gas phase composition of methane-bearing aqueous fluids from 273 to 523 K and from 1 to 2000 bar, Geochim. Cosmochim. Acta 70 (2006) 3369–3386, https://doi.org/10.1016/j.gca.2006.03.018.

[13] J. Rocha-Rios, R. Muñoz, S. Revah, Effect of silicone oil fraction and stirring rate on methane degradation in a stirred tank reactor, J. Chem. Technol. Biotechnol. 85 (2010) 314–319, https://doi.org/10.1002/JCTB.2339.

[14] S. Cantera, J.M. Estrada, R. Lebrero, P.A. Garc ıa-Encina, R. Muñoz, Comparative performance evaluation of conventional and two-phase hydrophobic stirred tank reactors for methane abatement: mass transfer and biological considerations, Biotechnol. Bioeng. 113 (2016) 1203–1212, https://doi.org/10.1002/bit.25897/abstract.

[15] Y. Rodríguez, P.I.M. Firmino, V. Pérez, R. Lebrero, R. Muñoz, Biogas valorization via continuous polyhydroxybutyrate production by Methylocystis hirsuta in a bubble column bioreactor, Waste Manag 113 (2020) 395–403, https://doi.org/10.1016/J.WASMAN.2020.06.009.

[16] R. Muñoz, A.J. Daugulis, M. Hernández, G. Quijano, Recent advances in two-phase partitioning bioreactors for the treatment of volatile organic compounds, Biotechnol. Adv. 30 (2012) 1707–1720, https://doi.org/10.1016/J.BIOTECHADV.2012.08.009.

[17] M.T. Kreutzer, F. Kapteijn, J.A. Moulijn, S. Ebrahimi, R. Kleerebezem, M.C.M. Van Loosdrecht, Monoliths as biocatalytic reactors: smart gas-liquid contacting for process intensification, Ind. Eng. Chem. Res. 44 (2005) 9646–9652, https://doi.org/10.1021/ie050286m.

[18] J. Rocha-Rios, N.J.R. Kraakman, R. Kleerebezem, S. Revah, M.T. Kreutzer, M.C. M. van Loosdrecht, A capillary bioreactor to increase methane transfer and oxidation through Taylor flow formation and transfer vector addition, Chem. Eng. J. 217 (2013) 91–98, https://doi.org/10.1016/J.CEJ.2012.11.065.

[19] C.R. Cattaneo, Y. Rodríguez, E.R. Rene, O. García-Depraect, R. Muñoz, Biogas bioconversion into poly(3-hydroxybutyrate) by a mixed microbial culture in a novel Taylor flow bioreactor, Waste Manag 150 (2022) 364–372, https://doi.org/10.1016/J.WASMAN.2022.07.017.

[20] A. Etminan, Y.S. Muzychka, K. Pope, A review on the hydrodynamics of taylor flow in microchannels: experimental and computational studies, Process. 2021, Vol. 9, Page 870 9 (2021) 870, https://doi.org/10.3390/PR9050870.

[21] N.J.R. Kraakman, J. González-Martín, C. Pérez, E. Rodríguez, R. Lebrero, M. A. Deshusses, R. Muñoz, Hydrophobic air pollutants removal at one second gas contact in a multi-channel capillary bioreactor, J. Environ. Chem. Eng. 11 (2023) 110502, https://doi.org/10.1016/J.JECE.2023.110502.

[22] A.D. Eaton, M.A.H. Franson, L.S. Clesceri, E.W. Rice, A.E. Greenberg, Standard methods for the examination of water & wastewater, (2005) 1.v-1.v.

[23] V.N. Khmelenina, M.G. Kalyuzhnaya, N.G. Starostina, N.E. Suzina, Y.A. Trotsenko, Isolation and characterization of halotolerant alkaliphilic methanotrophic bacteria from Tuva soda lakes, Curr. Microbiol. 35 (1997) 257–261, https://doi.org/10.1007/S002849900249/METRICS.

[24] Á. Kis, K. Laczi, A. Hakdú, Á. Szilágyi, G. Rákhely, K. Perei, Efficient Removal of Unctuous Wastes from Wastewater, Int. J. Biosci. Biochem. Bioinforma. 3 (2013) https://www.researchgate.net/publication/281775217_Efficient_Removal_of_Unctuous_Wastes_from_Wastewater.

[25] J.R. Ottoni, S.P.F. Bernal, T.J. Marteres, F.N. Luiz, V.P. dos Santos, Â.G. Mari, J. G. Somer, V.M. de Oliveira, M.R.Z. Passarini, Cultured and uncultured microbial community associated with biogas production in anaerobic digestion processes, Arch. Microbiol. 204 (2022), https://doi.org/10.1007/S00203-022-02819-8.

[26] A. Pandey, M. De, Significant hydrogen production by Enterococcus faecium IITGEN1 and Proteus mirabilis IITGEN2 newly isolated from local waste sources, Int. J. Environ. Sci. Technol. (2024), https://doi.org/10.1007/S13762-024-05844-W.

[27] S. Cantera, E. Rodríguez, N. Santaella Vecchini, J.C. López, P.A. García-Encina, D. Z. Sousa, R. Muñoz, Resilience and robustness of alphaproteobacterial methanotrophs upon methane feast-famine scenarios, Environ. Res. 239 (2023) 117376, https://doi.org/10.1016/J.ENVRES.2023.117376.

[28] T. García-Pérez, J.C. López, F. Passos, R. Lebrero, S. Revah, R. Muñoz, Simultaneous methane abatement and PHB production by Methylocystis hirsuta in a novel gas-recycling bubble column bioreactor, Chem. Eng. J. 334 (2018) 691–697, https://doi.org/10.1016/J.CEJ.2017.10.106.

[29] R. Lebrero, L. Hernández, R. Pérez, J.M. Estrada, R. Muñoz, Two-liquid phase partitioning biotrickling filters for methane abatement: exploring the potential of hydrophobic methanotrophs, J. Environ. Manag. 151 (2015) 124–131, https://doi.org/10.1016/J.JENVMAN.2014.12.016.

[30] J.C. López, L. Merchán, R. Lebrero, R. Muñoz, Feast-famine biofilter operation for methane mitigation, J. Clean. Prod. 170 (2018) 108–118, https://doi.org/10.1016/J.JCLEPRO.2017.09.157.

[31] V.N. Khmelenina, V.G. Sakharovskii, A.S. Reshetnikov, Y.A. Trotsenko, Synthesis of osmoprotectants by halophilic and alkaliphilic methanotrophs, Orig. Russ. Text.

Copyr. 69 (2000) 465–470, https://link.springer.com/content/pdf/10.1007/BF02756759.pdf (accessed June 22, 2022).
[32] S. Cantera, S. Bordel, R. Lebrero, J. Gancedo, P.A. García-Encina, R. Muñoz, Bioconversion of methane into high profit margin compounds: an innovative, environmentally friendly and cost-effective platform for methane abatement, World J. Microbiol. Biotechnol. 35 (2019), https://doi.org/10.1007/S11274-018-2587-4.
[33] A.M. AlSayed Mahmoud, Biological conversion process of methane into methanol using mixed culture methanotrophic bacteria enriched from activated sludge system, York university, 2017. https://www.researchgate.net/publication/330259641_BIOLOGICAL_CONVERSION_PROCESS_OF_METHANE_INTO_METHANOL_USING_MIXED_CULTURE_METHANOTROPHIC_BACTERIA_ENRICHED_FROM_ACTIVATED_SLUDGE_SYSTEM (accessed February 8, 2024).
[34] J.M. Walter, L.S. de Oliveira, D.A. Tschoeke, P.M. Meirelles, M.H.C.B. Neves, D. Batista, A.P. Carvalho, R.Dos Santos Costa, S. Dobretsov, R. Coutinho, J. Swings, C.C. Thompson, F.L. Thompson, Metagenomic insights into ecosystem function in the microbial mats of a large hypersaline coastal lagoon system, Front. Mar. Sci. 8 (2021) 715335, https://doi.org/10.3389/FMARS.2021.715335/BIBTEX.
[35] A.S. Reshetnikov, V.N. Khmelenina, I.I. Mustakhimov, Y.A. Trotsenko, Genes and enzymes of ectoine biosynthesis in halotolerant methanotrophs, Methods Enzym. 495 (2011) 15–30, https://doi.org/10.1016/B978-0-12-386905-0.00002-4.
[36] S. Cantera, I. Sánchez-Andrea, L.J. Sadornil, P.A. García-Encina, A.J.M. Stams, R. Muñoz, Novel haloalkaliphilic methanotrophic bacteria: an attempt for enhancing methane bio-refinery, J. Environ. Manag. 231 (2019) 1091–1099, https://doi.org/10.1016/J.JENVMAN.2018.11.017.
[37] C.K. Arya, S. Maurya, G. Ramanathan, Insight into the metabolic pathways of Paracoccus sp. strain DMF: a non-marine halotolerant methylotroph capable of degrading aliphatic amines/amides, Environ. Sci. Pollut. Res. 30 (2023) 125947–125964, https://doi.org/10.1007/S11356-023-30858-1/FIGURES/1.
[38] J. Piontek, C. Meeske, C. Hassenrück, A. Engel, K. Jürgens, Organic matter availability drives the spatial variation in the community composition and activity of Antarctic marine bacterioplankton, Environ. Microbiol. 24 (2022) 4030–4048, https://doi.org/10.1111/1462-2920.16087.